



HAL
open science

Mathematical analysis of whispering gallery modes in graded index optical micro-disk resonators

Stéphane Balac, Monique Dauge, Yannick Dumeige, Patrice Féron, Zoïs Moitier

► **To cite this version:**

Stéphane Balac, Monique Dauge, Yannick Dumeige, Patrice Féron, Zoïs Moitier. Mathematical analysis of whispering gallery modes in graded index optical micro-disk resonators. The European Physical Journal D: Atomic, molecular, optical and plasma physics, 2020, 74 (11), pp.# 221. 10.1140/epjd/e2020-10303-5 . hal-02157635v2

HAL Id: hal-02157635

<https://hal.science/hal-02157635v2>

Submitted on 4 Sep 2020

HAL is a multi-disciplinary open access archive for the deposit and dissemination of scientific research documents, whether they are published or not. The documents may come from teaching and research institutions in France or abroad, or from public or private research centers.

L'archive ouverte pluridisciplinaire **HAL**, est destinée au dépôt et à la diffusion de documents scientifiques de niveau recherche, publiés ou non, émanant des établissements d'enseignement et de recherche français ou étrangers, des laboratoires publics ou privés.

Mathematical analysis of whispering gallery modes in graded index optical micro-disk resonators

Stéphane Balac¹, Monique Dauge¹, Yannick Dumeige², Patrice Féron², and Zoïa Moitier¹

¹ UNIV. RENNES, CNRS, IRMAR - UMR 6625, F-35000 Rennes, France

² UNIV. RENNES, CNRS, FOTON-UMR 6082, Enssat, F-22305 Lannion, France

Received: date / Revised version: date

Abstract. We study from a theoretical point of view whispering gallery modes (WGM) in graded index micro-disk resonators where the refractive optical index varies with the radial position. Using a quantum mechanical analogy, we highlight three different behaviors for the WGM depending on the sign of a key parameter expressed as the ratio of the refractive index value to its derivative at the cavity boundary. This results in three asymptotic expansions of the resonances for large polar mode index providing first-approximations of WGM in a simple and quick way. Besides, these expansions yield a theoretical foundation to considerations of Ilchenko et al. in J. Opt. Soc. Am. A **20**, 157 (2003), about three sorts of effective potentials for TE modes in a dielectric sphere.

PACS. 42.55.Sa Microcavity and microdisk lasers – 42.25.Bs Wave propagation, transmission and absorption – 02.30.Mv Approximations and expansions

1 Introduction

Optical micro-resonators are key devices for many applications in photonics and they have been widely studied in the past two decades [1,2]. Optical dielectric resonators supporting Whispering Gallery Modes (WGM) have gained much interest thanks to their capability to strongly confine the light in very compact volumes with exceptional properties like a very narrow spectral linewidth and high quality factor. WGM resonators are usually formed of dielectric materials with a constant refractive index. This results in a complex spectral pattern with unequal mode spacing and a high spectral density that may potentially limit their performance or the range of their applications. Optical micro-resonators with spatially varying refractive index offer new opportunities to improve or enlarge the field of applications of optical micro-resonators. This kind of optical micro-cavities falls under the category of Graded index (GRIN) structures that are widely used in various fields in optics [3].

WGM in optical micro-resonators are specific resonances of electromagnetic waves inside a convex micro-metric dielectric cavity with smooth surface. They correspond to light-waves circling around the cavity, almost perfectly guided round by optical total internal reflection, that meet a resonance condition (after one round-trip they return to the same point with the same phase and hence interfere constructively with themselves, forming standing waves). Use of graded index cavity can result in a shift of the spatial location of WGM away from the exterior surface of the resonator towards the interior of the resonator. This can reduce the overall optical loss at the exterior surface caused by adverse effects of surface contamination and roughness. It may also produce optical spectra of WGM that

are different from the one produced by WGM resonators with constant refractive indices, e.g. equally spaced resonances.

Among the graded index structures, a modified form of “Maxwell’s fish eye” has been studied in [4,5]. The authors investigated by numerical simulation the features of WGM in a 2D graded index micro-disk (with radius R) where refractive index varies according to the radial position r as

$$n(r) = \frac{n_0}{1 + \frac{r^2}{R^2}}.$$

In [6] the authors consider a micro-cavity made by a quadratic-index glass, doped with dye molecules, and the refractive index is written as $n(r) = n_0 - \frac{1}{2}n_2r^2$, where $n_2 > 0$. In [7] the authors investigate graded index micro-spheres and they consider the case of an refractive index varying according to the radial position r as

$$n(r) = \sqrt{n_0^2 + \varepsilon'(R-r)}$$

where $n_0 > 1$ and $\varepsilon' > 0$ has unit μm^{-1} .

In this paper, we investigate from a mathematical point of view WGM in a graded index micro-disk where the refractive index n varies with the radial position r in a general way and we highlight three different behaviors for the WGM depending on the features of the refractive index at the cavity boundary. Moreover, we characterize for each of these three cases the resonance wave-numbers and modes through asymptotic expansions providing first-approximations of WGM wave-numbers and modes and a first-insight into the expected behavior of WGM in such optical devices.

We assume here a 2D setting for the micro-disk and therefore vertical effects such as mode confinement are neglected.

We denote by Ω the bi-dimensional dielectric micro-disk cavity and by R its radius. As well known [2] for such a bi-dimensional resonance problem, the mode corresponding to a resonance is either a transverse electric (TE) field or a transverse magnetic (TM) one and the resonance problem takes two different forms according to whether one is interested in the TE or TM modes, see Appendix A for details. Moreover, it is well known that the resonance wave-numbers k are complex numbers with a negative imaginary part under the $e^{-i\omega t}$ convention for harmonic time dependence of the electromagnetic field. The results presented here enter a more general mathematical framework the details of which can be found in [8, 9].

We denote by $L^2_{\text{loc}}(\mathbb{R}^2)$ the Lebesgue set of locally square integrable functions in \mathbb{R}^2 and by $H^2(\Omega)$ (resp. $H^2_{\text{loc}}(\mathbb{C}\Omega)$) the Sobolev space of square integrable (resp. locally square integrable) functions in Ω (resp. $\mathbb{C}\Omega$) with all derivatives up to order 2 in $L^2(\Omega)$ (resp. $L^2_{\text{loc}}(\mathbb{C}\Omega)$). We introduce the space of functions

$$D(\mathbb{R}^2) = \{u \in L^2_{\text{loc}}(\mathbb{R}^2) \mid u|_{\Omega} \in H^2(\Omega), u|_{\mathbb{C}\Omega} \in H^2_{\text{loc}}(\mathbb{C}\Omega)\}.$$

For a varying refractive index n , the resonance problems for TE and TM modes in the cavity Ω can be gathered into a unique form by introducing a mode selection index p such that $p = 1$ for TM modes and $p = -1$ for TE modes, see Appendix A for details. This resonance problem reads: find $(k, u) \in \mathbb{C} \times D(\mathbb{R}^2)$ such that $u \neq 0$, $\Im(k) < 0$ and

$$-\operatorname{div}(n^{p-1} \nabla u) - k^2 n^{p+1} u = 0 \quad \text{in } \Omega \text{ and } \mathbb{C}\Omega \quad (1a)$$

$$[u] = 0 \quad \text{across } \Gamma \quad (1b)$$

$$\left[n^{p-1} \frac{\partial u}{\partial \nu} \right] = 0 \quad \text{across } \Gamma \quad (1c)$$

where Γ denotes the boundary of Ω , ν the outward unit normal to Γ and the brackets indicate the jump across Γ of the quantity inside the brackets. Note that throughout the paper, in the exterior domain the refractive index n is assumed to be 1. The out-going wave condition at infinity uses polar coordinates (r, θ) centered at the center of the disk Ω and reads: $\forall r > R \forall \theta \in [0, 2\pi]$ there exists $(c_m)_{m \in \mathbb{Z}}$ such that in the polar coordinates system (r, θ)

$$u(r, \theta) = \sum_{m \in \mathbb{Z}} c_m H_m^{(1)}(kr) e^{im\theta} \quad (1d)$$

where $H_m^{(1)}$ denotes Hankel's function of the first kind and order m and $(c_m)_{m \in \mathbb{Z}}$ belongs to the space of complex valued square-summable sequences $\ell^2(\mathbb{C})$. For a short and very understandable introduction to mathematical aspects of resonance problems, we refer to [10].

For TE modes, in the cylindrical basis, the unknown u is the component H_z of the magnetic field and the other two non-zero components of the electromagnetic field are given by

$$E_r(r, \theta) = \frac{i}{\omega \epsilon_0 n^2} \frac{1}{r} \partial_\theta H_z(r, \theta),$$

$$E_\theta(r, \theta) = -\frac{i}{\omega \epsilon_0 n^2} \partial_r H_z(r, \theta).$$

For TM modes, in the cylindrical basis, the unknown u is the component E_z of the magnetic field and the other two non-zero

components of the electromagnetic field are given by

$$H_r(r, \theta) = \frac{1}{i\omega\mu_0} \frac{1}{r} \partial_\theta E_z(r, \theta),$$

$$H_\theta(r, \theta) = -\frac{1}{i\omega\mu_0} \partial_r E_z(r, \theta).$$

The wave-numbers k are complex with negative imaginary parts due to the leakage. The quantity $2\pi/\Re(k)$ gives the resonance wavelength, whereas the imaginary part of k corresponds to the photon lifetime τ in the cavity through the relation $\tau = -\frac{1}{2c\Im(k)}$. Moreover, the radiative quality factor of the mode is defined as $Q = \frac{\Re(k)}{2\Im(k)}$. Note that the above problem setting is actually applicable to any shape for the 2D cavity and for any position dependent refractive index n in the cavity.

The paper is organized as follows. In Section 2, we show from the system of equations (1a)-(1d) how some of the features of resonances in a micro-disk cavity with a radially varying refractive index can be obtained by using some semi-classical analysis techniques for Schrödinger operators associated with some effective potentials. This study results in asymptotic expansions for large polar mode index m providing first order approximations for resonances and modes in three distinct and well defined cases. Finally, in Section 3, we assess the accuracy of our asymptotic formulas for WGM resonances in a micro-disk by comparison with values obtained when solving problem (1) by a numerical method.

It is interesting to note that the splitting into three cases according to the behavior of the minimum of an effective potential has been already highlighted in [7] in the case of a micro-sphere. In fact, our formulas for TM modes in a disk apply directly to the case of TE modes in a graded index micro-sphere investigated in [7] through an elementary change of polar mode index. In Appendix C, we show how our analysis complements and strengthens the considerations of [7] who gives a two-term asymptotics only in the first one of the three cases.

2 Resonances in a disk cavity with a radially varying refractive index

2.1 Schrödinger analogy

When considering a disk-shaped cavity with a radially varying refractive index n , the Fourier approach can be used to solve the resonance problem (1). The eigenfunction u for a solution (k, u) to problem (1) is expanded in polar coordinates as

$$u(r, \theta) = \sum_{m \in \mathbb{Z}} u_m(r) e^{im\theta} \quad (2)$$

and solutions to problem (1) are obtained from the solutions of the following family of 1D problems: Find $(k, u_m) \in \mathbb{C} \times$

$D(\mathbb{R}^+, r dr)$ such that $\Im(k) < 0$, $u_m \neq 0$ and

$$u_m''(r) + \left(\frac{1}{r} + (p-1)\frac{n'(r)}{n(r)}\right)u_m'(r) \quad (3a)$$

$$+ \left(k^2 n^2 - \frac{m^2}{r^2}\right)u_m(r) = 0 \quad \text{in }]0, R[\text{ and }]R, +\infty[$$

$$[u_m(R)] = 0 \quad (3b)$$

$$\left[n^{p-1}(R)u_m'(R)\right] = 0 \quad (3c)$$

$$u_m(r) \propto H_m^{(1)}(kr) \text{ as } r \rightarrow +\infty \quad (3d)$$

where $D(\mathbb{R}^+, r dr) = \{u \in L_{\text{loc}}^2(\mathbb{R}^+, r dr) \mid u|_{]0, R[} \in H^2(]0, R[, r dr), u|_{]R, +\infty[} \in H_{\text{loc}}^2(]R, +\infty[, r dr)\}$ (the notation $r dr$ refers to the measure on the Lebesgue space). Actually, the formulation of problem (3) holds for $m \neq 0$, whereas for $m = 0$ the additional Neumann boundary condition $u_m'(0) = 0$ must be added to have a well-posed problem. A solution (k_m, u_m) to problem (3) is referred to as a mode of the micro-disk cavity with *polar mode index* m . For a given mode index m , problem (3) has a sequence of solutions, indexed by a second index $j \in \mathbb{N}$, termed the *radial mode index*. Moreover, one can see from problem (3) that in a GRIN micro-disk resonator the resonances have multiplicity 2 since the two indexes $\pm m$ provide the same resonance wave-number k , the modes being expressed as a linear combination of $u_m(r)e^{im\theta}$ and its complex conjugate $\overline{u_m(r)}e^{-im\theta}$.

A qualitative study of the resonances, solutions to problem (3), can be achieved by using semi-classical analysis techniques for the solution of some stationary Schrödinger equations. To this end, we set $h = 1/m$ and $\gamma = n_0^2 k^2 / m^2$ where

$$n_0 = \lim_{r \nearrow R} n(r)$$

is the value of the refractive index at the inner boundary of the cavity ($n_0 > 1$). With these notations, equation (3a) can be reformulated as the following radial Schrödinger equation

$$-h^2 \mathcal{L}u_m + Vu_m = \gamma u_m \quad (4)$$

where \mathcal{L} denotes the elliptic linear differential operator

$$\begin{aligned} \mathcal{L} &= \frac{n_0^2}{n^2(r)} \left(\partial_{rr}^2 + \frac{1}{r} \partial_r + (p-1) \frac{n'(r)}{n(r)} \partial_r \right) \\ &= \frac{n_0^2}{rn^{p+1}(r)} \partial_r (rn^{p-1}(r) \partial_r) \end{aligned} \quad (5)$$

and the potential energy function V is defined by

$$V(r) = \frac{n_0^2}{r^2 n(r)^2}. \quad (6)$$

The linear operator \mathcal{L} is self-adjoint on the space $L_{\rho}^2(\mathbb{R}^+)$ of square integrable functions for the measure $\rho = n^{p+1}(r)r dr$. Moreover, since $\lim_{r \nearrow R} V(r) = \frac{1}{R^2}$ and $\lim_{r \searrow R} V(r) = \frac{n_0^2}{R^2} > \frac{1}{R^2}$, we have a potential barrier at $r = R$.

As we are interested in WGM, the angular mode index m is large and among the solutions (k_m, u_m) to problem (3) for such a m , we are interested in solutions such that the mode u_m is ‘‘concentrated’’ inside the cavity, in a vicinity of the disk

boundary. As a consequence, the parameter h is a small positive parameter and our study falls under the semi-classical regime for the Schrödinger equation. In this framework, we are interested in solutions to the Schrödinger equation that concentrate around the local minimum in $(0, R]$ of the potential V the closest to R . Thus, we must consider the sign of $V'(R) = -\frac{2}{R^2} \kappa$ where

$$\kappa = \frac{1}{R} + \frac{n_1}{n_0} \quad \text{with} \quad n_1 = \lim_{r \nearrow R} n'(r). \quad (7)$$

We have identified three typical behaviors depending on the sign of κ , see Fig. 1.

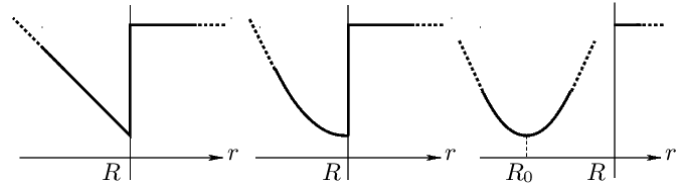


Fig. 1. The three typical local behaviors of the potential V : From left to right, half-triangular well ($\kappa > 0$), half-quadratic well ($\kappa = 0$) and quadratic well ($\kappa < 0$).

a) Half-triangular potential well. If $\kappa > 0$ then V is decreasing in a left neighborhood of R and has a local minimum at R . The special case of a disk cavity with constant index enters this heading. The quantum mechanism analogy is similar to the one given in Appendix B for a disk cavity with constant index.

b) Half-quadratic potential well. If $\kappa = 0$, under the additional condition $\mu > 0$, where

$$\mu = \frac{2}{R^2} - \frac{n_2}{n_0} \quad \text{with} \quad n_2 = \lim_{r \nearrow R} n''(r), \quad (8)$$

the potential V has a local minimum at R . The modified form of Maxwell’s fish eye GRIN structure investigated in [4] enters this heading.

c) Internal quadratic potential well. If $\kappa < 0$, the effective potential V has at least one local minimum R_0 in $(0, R)$ since $\lim_{r \searrow 0} V(r) = +\infty$. Under the additional condition $\mu = \frac{2}{R_0^2} - \frac{n''(R_0)}{n(R_0)} > 0$, the potential is quadratic in a neighborhood of the minimum. The advantage of cavities with such refractive index is that the modes are located slightly inside the cavity and therefore the resonances are less sensitive to edge defects of the cavity.

Note that the above list of cases is not exhaustive, but the other cases impose strong conditions on the refractive index function n which would be questionable in terms of technological design. Note also that the potential V may have several local minima in $]0, R]$, around which resonant modes may locate themselves, but they are of less practical interest.

2.2 Principles of construction of asymptotic formulas for resonances

In order to find approximate solutions to system (3), we consider the Schrödinger equation (4) and perform a Taylor expan-

sion of its coefficients at the point where the potential V has its minimum. In cases a) and b) this point is $r = R$, and in case c) it is $r = R_0$. Let us explain the principles in cases a) and b) before giving more details in the corresponding sections. We perform the change of variables $r \mapsto \xi = \frac{r}{R} - 1$ sending R to 0 and write equation (4) with this coordinate: For \mathcal{L} we obtain the following expression

$$\frac{n_0^2}{R^2 n^2 (R + R\xi)} \left(\partial_{\xi\xi}^2 + \frac{R}{R+R\xi} \partial_{\xi} + (p-1) \frac{Rn_1'(R+R\xi)}{n(R+R\xi)} \partial_{\xi} \right)$$

whereas for the potential V we obtain $\frac{n_0^2}{(R+R\xi)^2 n(R+R\xi)^2}$. Then, considering a Taylor expansion at the order 0 in $\xi = 0$ of the operator \mathcal{L} coefficients, we find

$$\mathcal{L} \simeq \begin{cases} \frac{1}{R^2} (\partial_{\xi\xi}^2 + \partial_{\xi} + (p-1) \frac{Rn_1}{n_0} \partial_{\xi}) & \xi < 0 \\ \frac{n_0^2}{R^2} (\partial_{\xi\xi}^2 + \partial_{\xi}) & \xi > 0 \end{cases}$$

For the potential V , a Taylor expansion at the order 2 in $\xi = 0$ will be sufficient in any case:

$$V \simeq \begin{cases} \frac{1}{R^2} - \frac{2}{R} \kappa \xi + (3\kappa^2 - 2\kappa + \mu) \xi^2 & \xi < 0 \\ \frac{n_0^2}{R^2} & \xi > 0 \end{cases}$$

where the quantities κ and μ were introduced in (7) and (8). As for the ‘‘eigenvalue’’ γ in (4), we look for a quantity close to the bottom of the potential well at $\xi = 0$, i.e.

$$\gamma = \frac{1}{R^2} (1 + \tilde{\gamma}) \quad \text{with} \quad \lim_{h \rightarrow 0} \tilde{\gamma} = 0.$$

With these approximations, equation (4) outside the cavity, i.e. for positive ξ , becomes

$$-h^2 n_0^2 (\partial_{\xi\xi}^2 + \partial_{\xi}) \varphi + (n_0^2 - 1) \varphi = \tilde{\gamma} \varphi$$

and, at the limit $h = 0$, we find $\frac{n_0^2 - 1}{R^2} \varphi = 0$, i.e. $\varphi = 0$ for $\xi > 0$. Hence the jump condition (3b) across $r = R$ ($\xi = 0$) implies that the approximate solution inside the cavity should satisfy the Dirichlet condition $\varphi(0) = 0$.

From this point, the study of the three cases differentiates.

2.3 Asymptotic formulas for resonances in the half-triangular potential well case

Let us consider first the case of a half-triangular potential well where $\kappa > 0$. Neglecting here the term of order 2 in the Taylor expansion of V , our approximate equation inside the cavity ($\xi < 0$) can be written as

$$-h^2 (\partial_{\xi\xi}^2 + \partial_{\xi} + (p-1) \frac{Rn_1}{n_0} \partial_{\xi}) \varphi - 2R \kappa \xi = \tilde{\gamma} \varphi \quad (9)$$

with the Dirichlet condition $\varphi(0) = 0$. In order to homogenize the principal terms $-h^2 \partial_{\xi\xi}^2$ and $-\kappa \xi$, we introduce the scaled variable σ defined by [11] $\sigma = h^{-\frac{2}{3}} \xi$ and the new unknown

$v(\sigma) = \varphi(\sigma h^{\frac{2}{3}})$. The approximate Schrödinger equation (9) for φ gives rise to the following ODE for v (posed on $(-\infty, 0)$ with $v(0) = 0$):

$$-h^{\frac{2}{3}} \left(v''(\sigma) + 2R\kappa \sigma v(\sigma) \right) + h^{\frac{4}{3}} \left(1 + (p-1) \frac{Rn_1}{n_0} \right) v'(\sigma) = \tilde{\gamma} v(\sigma). \quad (10)$$

By considering a formal series expansion for v in the form

$$v(\sigma) = v_0(\sigma) + h^{\frac{1}{3}} v_1(\sigma) + h^{\frac{2}{3}} v_2(\sigma) + \dots$$

and $\tilde{\gamma} = \gamma_2 h^{\frac{2}{3}} + \gamma_3 h + \gamma_4 h^{\frac{4}{3}} + \dots$ for the eigenvalue, and by plugging these expressions into (10) and equating terms with the same order in h , one obtains that v_0 satisfies

$$-v_0''(\sigma) - 2\check{\kappa} \sigma v_0(\sigma) = \gamma_2 v_0(\sigma), \quad \text{with} \quad \check{\kappa} = R\kappa.$$

By making the substitution $X = (2\check{\kappa})^{\frac{1}{3}} \sigma + (2\check{\kappa})^{-\frac{2}{3}} \gamma_2$, it is found that $V(X) \equiv v_0(\sigma)$ solves the reverse Airy equation

$$-V'' + XV = 0$$

and we deduce that $v_0(\sigma) = A((2\check{\kappa})^{\frac{1}{3}} \sigma + (2\check{\kappa})^{-\frac{2}{3}} \gamma_2)$ where A denotes the mirror symmetric Airy function $A : X \in \mathbb{R} \mapsto \text{Ai}(-X)$. The Dirichlet condition $v_0(0) = 0$ implies that there exists an integer $j \geq 0$ such that

$$(2\check{\kappa})^{-\frac{2}{3}} \gamma_2 = a_j$$

where $(a_j)_{j \geq 0}$ denotes the increasing sequence of the zeros of A . Hence $v_0(\sigma) = A(a_j + (2\check{\kappa})^{\frac{1}{3}} \sigma)$.

Finally, for the half-triangular potential well, the resonance corresponding to the polar mode index m and radial mode index $j \geq 0$ is found to have an asymptotic expansion in the form

$$k_{m,j} = \frac{m}{Rn_0} \left(1 + \frac{1}{2} (2\check{\kappa})^{\frac{2}{3}} a_j m^{-\frac{2}{3}} + \mathcal{O}(m^{-1}) \right) \quad (11)$$

and the corresponding mode inside the cavity (i.e. for $r < R$) satisfies

$$u_{m,j}(r) = A(a_j + (2\check{\kappa})^{\frac{1}{3}} m^{-\frac{2}{3}} \frac{r-R}{R}) + \mathcal{O}(m^{-\frac{1}{3}}).$$

We wish to draw attention to the fact that the so-called ‘‘radial mode index’’ j , introduced here as the index of the increasing sequence of the zeros of the reverse Airy’s function A can be interpreted as the number of sign changes (or nodal points) of the real part of a mode inside the cavity as illustrated in Section 3.

These formulas for the resonance $k_{m,j}$ and the mode $u_{m,j}$ are coherent with the first term of the known asymptotic expansion in a disk cavity with constant index, see e.g. [12]. It can be noted that the approximation obtained for the resonances and modes do not distinguish between TE and TM modes. The asymptotic developments have to be continued at a higher order to distinguish one from another. It can also be noted that one would obtain the same 2-term asymptotic expansion (11) for the Dirichlet problem in a disk as encountered e.g. in the closed

billiard problem in a circular dielectric cavity [13]. The distinction between the Dirichlet problem in a disk and the transmission problem (3) for a disk arises with the next terms in the asymptotic expansion. It is indeed possible, taking into account higher order Taylor expansions of V and of the coefficients of \mathcal{L} , and including the jump relation (3c) on first derivatives at $r = R$, to pursue the construction of approximate resonance pairs (k, u_m) up to an arbitrary precision, see [8, 9], but this goes beyond the scope of this paper. In particular, we obtained the following 4-term expansion:

$$k_{m,j} = \frac{m}{Rn_0} \left(1 + \frac{1}{2}(2\check{\kappa})^{\frac{2}{3}} a_j m^{-\frac{2}{3}} - \check{\kappa} n_0^p \frac{1}{\sqrt{n_0^2 - 1}} m^{-1} + \frac{1}{15}(2\check{\kappa})^{\frac{4}{3}} a_j^2 \left(\frac{17}{8} - \frac{3}{\check{\kappa}} + \frac{\check{\mu}}{\check{\kappa}^2} \right) m^{-\frac{4}{3}} + \mathcal{O}(m^{-\frac{5}{3}}) \right) \quad (12)$$

where $\check{\mu} = R^2 \mu$. One can see that the third term differs whether the resonance corresponds to a TE mode ($p = -1$) or to a TM mode ($p = 1$). This term also differs from the one obtained for the Dirichlet problem in a disk.

2.4 Asymptotic formulas for resonances in the half-quadratic potential well case

Let us now consider the half-quadratic potential well. In this case κ is zero and our approximate equation inside the cavity ($\xi < 0$) can be written as

$$-h^2 (\partial_{\xi}^2 + \partial_{\xi} + (p-1) \frac{Rn_1}{n_0} \partial_{\xi}) \varphi + \mu \xi^2 = \tilde{\gamma} \varphi \quad (13)$$

with the Dirichlet condition $\varphi(0) = 0$. Now we have to homogenize the principal terms $-h^2 \partial_{\xi}^2$ and $\mu \xi^2$. We introduce the scaled variable [11] $\sigma = h^{-\frac{1}{2}} \xi$ and the new unknown $v(\sigma) = \varphi(\sigma h^{\frac{1}{2}})$. The approximate Schrödinger equation (13) for φ gives rise to the following ODE for v (posed on $(-\infty, 0)$ with $v(0) = 0$):

$$h \left(-v''(\sigma) + \mu \sigma^2 v(\sigma) \right) + h^{\frac{3}{2}} \left(1 + (p-1) \frac{Rn_1}{n_0} \right) v'(\sigma) = \tilde{\gamma} v(\sigma). \quad (14)$$

The adapted formal series expansions for v and $\tilde{\gamma}$ involve now powers of $h^{\frac{1}{2}}$: $v(\sigma) = v_0(\sigma) + h^{\frac{1}{2}} v_1(\sigma) + \dots$ and $\tilde{\gamma} = \gamma_2 h + \gamma_3 h^{\frac{3}{2}} + \dots$. By plugging these expressions into (14) and equating terms with the same order in h , one obtains that v_0 satisfies

$$-v_0''(\sigma) + \check{\mu} \sigma^2 v_0(\sigma) = \gamma_2 v_0(\sigma)$$

where $\check{\mu} = R^2 \mu$. By making the substitution $X = \check{\mu}^{\frac{1}{4}} \sigma$, it is found that $V(X) \equiv v_0(\sigma)$ solves the harmonic oscillator equation $-V'' + X^2 V = \check{\mu}^{-\frac{1}{2}} \gamma_2 V$ on $(-\infty, 0)$ with Dirichlet condition $V(0) = 0$. Its eigenfunctions are known as Hermite functions $\psi_{\ell}(X)$ [14, Chp.22] with odd index because of the Dirichlet condition. The associate eigenvalue is $2\ell + 1$. Hence $v_0(\sigma) = \psi_{2j+1}(\check{\mu}^{\frac{1}{4}} \sigma)$ where $j \geq 0$. Finally, for the half-quadratic potential well, the resonance corresponding to the polar mode index m and radial mode index j is found to satisfy

$$k_{m,j} = \frac{m}{Rn_0} \left(1 + \frac{4j+3}{2} \check{\mu}^{\frac{1}{2}} m^{-1} + \mathcal{O}(m^{-\frac{3}{2}}) \right) \quad (15)$$

and the mode inside the cavity (*i.e.* for $r < R$) satisfies

$$u_{m,j}(r) = \psi_{2j+1}(\check{\mu}^{\frac{1}{4}} m^{\frac{1}{2}} \frac{r-R}{R}) + \mathcal{O}(m^{-\frac{1}{2}}). \quad (16)$$

One important feature of resonances in the half-quadratic potential well case is that they are organized in an asymptotic lattice with constant step: The gap between two resonances with consecutive polar mode index m and $m+1$ and the same radial mode index j is found to be

$$k_{m+1,j} - k_{m,j} = \frac{1}{Rn_0} + \mathcal{O}(m^{-\frac{1}{2}})$$

whereas when m is fixed and j is incremented by 1, the gap between two resonances is found to be

$$k_{m,j+1} - k_{m,j} = \frac{2\check{\mu}^{\frac{1}{2}}}{Rn_0} + \mathcal{O}(m^{-\frac{1}{2}}).$$

2.5 Asymptotic formulas for resonances in the internal quadratic potential well case

For the internal quadratic potential well, the reasoning is similar to the case of the half-quadratic potential well with R replaced by R_0 where R_0 denotes the local minimum of V inside the cavity the closest to R . The only difference comes from the lack of boundary condition at R_0 since the potential minimum is not anymore on the boundary at R . The resonance corresponding to the polar mode index m and radial mode index j is found to satisfy

$$k_{m,j} = \frac{m}{R_0 n(R_0)} \left(1 + \frac{2j+1}{2} \check{\mu}^{\frac{1}{2}} m^{-1} + \mathcal{O}(m^{-\frac{3}{2}}) \right) \quad (17)$$

where $\check{\mu} = 2 - R_0^2 n''(R_0)/n(R_0)$, and the corresponding mode inside the cavity (*i.e.* for $r < R$) satisfies

$$u_{m,j}(r) = \psi_j(\check{\mu}^{\frac{1}{4}} m^{\frac{1}{2}} \frac{r-R_0}{R_0}) + \mathcal{O}(m^{-\frac{1}{2}}). \quad (18)$$

One can see that in the internal quadratic potential well too, resonances are organized in an asymptotic lattice with constant step. The main interest of designing optical cavities with a radially varying index n entering this heading is that the mode is slightly shift inside the cavity reducing its sensitivity to edge roughness (compare relations (16) and (18)).

3 Numerical investigations

We have written a program under MATLAB to compute WGM in graded index optical micro-disks with radial varying refractive optical index. The program can be obtained from the corresponding author. The program solves the radial problem (3) using the Finite Difference Method [15] where the first and second order derivatives are approached by the following second-order of accuracy central difference schemes (for a small step-size $\delta_r > 0$)

$$u'(r) \approx \frac{u(r+\delta_r) - u(r-\delta_r)}{2\delta_r}$$

$$u''(r) \approx \frac{u(r+\delta_r) - 2u(r) + u(r-\delta_r)}{\delta_r^2}$$

The unbounded exterior domain is truncated at a finite distance of the dielectric cavity boundary by using the Perfectly Matched Layer method (PML). Namely, we use the PML investigated in [16]. The Finite Difference scheme we have implemented under MATLAB is second order accurate. Note that we have chosen the Finite Difference Method for its simplicity for such a one-dimensional problem but we could have also used the Finite Element Method [17] as in [8,9].

3.1 Half-triangular potential well

First, to validate both our asymptotic formula (11) and our MATLAB program, we consider the case of a disk with a constant refractive index $n_0 = 1.45$. The disk radius is $R = 10 \mu\text{m}$. In the particular case of a constant refractive index, one can solve problem (3) analytically. The resonances k are found to be the zeros of the following non-linear equation referred to as the *modal equation* [8,9]

$$f_m(z) = \frac{H_{m-1}^{(1)}(z)}{H_m^{(1)}(z)} - n_0^p \frac{J_{m-1}(n_0 z)}{J_m(n_0 z)} + \frac{m}{z} (1 - n_0^{p-1}) = 0$$

where $p = 1$ for TM modes and $p = -1$ for TE modes and $z = kR = \frac{2\pi R}{\lambda}$. J_m refers to Bessel's function of the first kind. Moreover, the mode u_m for a given resonance k is found to be

$$u_m(r) = \begin{cases} \frac{J_m(n_0 k r)}{J_m(n_0 k R)} & \text{if } r \leq R \\ \frac{H_m^{(1)}(k r)}{H_m^{(1)}(k R)} & \text{if } r > R \end{cases}$$

We provide in Table 1 the first five resonance wavelengths $\lambda = 2\pi/k$ in μm for TE modes with polar mode index $m = 60$ computed by solving the modal equation $f_m(z) = 0$. The third column provides the residual, i.e. the absolute value of the modal function at resonance $|f_m(2\pi R/\lambda)|$ as an indicator of the accuracy of the zero finding method. We also provide in Table 2 the first five resonance wavelengths λ computed by our Finite Difference program with a step-size of $10^{-3} \mu\text{m}$. The third column indicates the relative error on the resonances compared to the ‘‘exact’’ ones provided in Table 1. We observe that four to five digits on the real part of the resonance are correct. Finally, we provide in Table 3 the first five resonance wavelengths λ computed by the asymptotic formula (11). The third column indicates the relative error on the resonances compared to the ‘‘exact’’ ones provided in Table 1. We can observe that the asymptotic formula (11) provides approximate values of the resonances with an error around 1% for that value of m . This can be considered as satisfactory for such a two-term asymptotic formula. It should be noted that the accuracy of the asymptotic formula (11) is strongly depend on the value of the mode index m : The larger m is, the more accurate is the approximation. (The remainder is in $\mathcal{O}(m^{-1})$.) For instance, for the same micro-disk, the average error on the first five resonance wavelengths for $m = 200$ is 0.23%. It should also be noted that the accuracy of the results for a fixed value of m could be improved by taking into account more terms in the asymptotic expansion as it is the case with the four-term asymptotic formula (12) with

a remainder in $\mathcal{O}(m^{-5/3})$. For instance, the average error on the first five resonance wavelengths falls to less than 0.75% when using formula (12).

1	$1.365519863852797 + i8.899057980609237 \cdot 10^{-9}$	$1.87 \cdot 10^{-16}$
2	$1.256150131337898 + i3.228526827244588 \cdot 10^{-6}$	$7.81 \cdot 10^{-15}$
3	$1.176783344038231 + i1.472899763865047 \cdot 10^{-4}$	$1.37 \cdot 10^{-14}$
4	$1.114014527345193 + i1.567378520103474 \cdot 10^{-3}$	$2.20 \cdot 10^{-14}$
5	$1.060466939160361 + i5.308036592118068 \cdot 10^{-3}$	$2.44 \cdot 10^{-14}$

Table 1. First five exact resonance wavelengths λ in μm for TE modes with polar mode index $m = 60$ for a micro-disk with constant refractive index $n_0 = 1.45$ and radius $R = 10 \mu\text{m}$. The third column provides the absolute value of the modal function at resonance $|f_m(2\pi R/\lambda)|$.

1	$1.365519834571472 + i8.620120805955066 \cdot 10^{-9}$	$2.14 \cdot 10^{-8}$
2	$1.256150084591846 + i3.115865384096499 \cdot 10^{-6}$	$9.71 \cdot 10^{-8}$
3	$1.176786476706345 + i1.480719183809064 \cdot 10^{-4}$	$2.74 \cdot 10^{-6}$
4	$1.113987662838273 + i1.566746482111717 \cdot 10^{-3}$	$2.41 \cdot 10^{-5}$
5	$1.060561414039830 + i5.279762347031864 \cdot 10^{-3}$	$9.29 \cdot 10^{-5}$

Table 2. First five resonance wavelengths λ in μm for TE modes obtained by our Finite Difference program. The third column indicates the relative error on the resonances compared to the ‘‘exact’’ ones provided in Table 1.

1	1.3544358	$8.12 \cdot 10^{-3}$
2	1.2531419	$2.40 \cdot 10^{-3}$
3	1.1808407	$3.45 \cdot 10^{-3}$
4	1.1235487	$8.67 \cdot 10^{-3}$
5	1.0758336	$1.53 \cdot 10^{-2}$

Table 3. First five resonance wavelengths λ in μm for TE modes obtained by the asymptotic formula (11). The third column indicates the relative error on the resonances compared to the ‘‘exact’’ ones provided in Table 1.

We have depicted in Fig. 2 the variations in the radial direction of the modulus of the mode u_m for the first resonance provided in Table 2 (top) and the 2D representation of the real part of $u_m(r) e^{im\theta}$ (bottom). Computations were achieved using our Finite Difference program under MATLAB.

3.2 Half-quadratic potential well

We now consider the case of a micro-disk with radius $R = 10 \mu\text{m}$ and refractive index varying according to the radial position r as $n(r) = \frac{2n_0}{1+r^2/R^2}$ where $n_0 = n(R) = 1.45$. This refractive index profile corresponds to the modified form of ‘‘Maxwell’s fish eye’’ GRIN studied in [4]. We have $n_1 = n'(R) = -n_0/R$ so

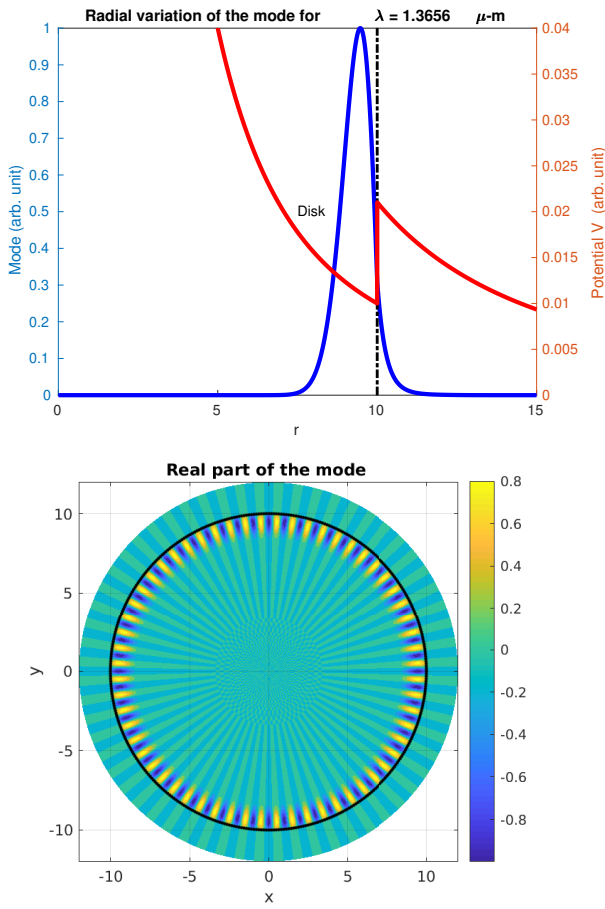


Fig. 2. Variation in the radial direction of the modulus of the mode u_m for the first resonance provided in Table 2 (top, blue line), potential V (top, red line) and 2D representation of the real part of $u_m(r)e^{im\theta}$ (bottom). The black circle indicates the disk boundary. The PML area is not represented.

that $\kappa = 0$ and this refractive index profile corresponds to the half-quadratic potential well.

We provide in Table 4 the first five resonance wavelengths λ in μm for TE modes with polar mode index $m = 60$ obtained by the asymptotic formula (11) (second column) and computed by our Finite Difference program (third column) with a step-size of $10^{-3} \mu\text{m}$. It can be noticed that compared to a dielectric cavity with constant refractive index, the resonances are more regularly spaced. This feature of resonances can be easily inferred from the asymptotic formula (15) for the half-quadratic potential well and it is not true for refractive index profile corresponding to half-triangular potential well, see (11).

We have depicted in Fig. 3 the variations in the radial direction of the modulus of the mode u_m for the first resonance provided in Table 4 (top) and the 2D representation of the real part of $u_m(r)e^{im\theta}$ (bottom).

We have also depicted in Fig. 4 the variations in the radial direction of the modulus of the mode u_m for the fifth resonance provided in Table 4 (top) and the 2D representation of the real part of $u_m(r)e^{im\theta}$ (bottom). It can be noted that the index j labeling the resonances in formula (11) (in reference to the in-

1	1.4814014	$1.4834423 + i3.4093579 \cdot 10^{-13}$
2	1.4347431	$1.4379203 + i2.7195200 \cdot 10^{-12}$
3	1.3909342	$1.3949026 + i4.2106368 \cdot 10^{-10}$
4	1.3497213	$1.3543145 + i4.7185218 \cdot 10^{-09}$
5	1.3108804	$1.3160060 + i4.2639670 \cdot 10^{-08}$

Table 4. First five resonance wavelengths λ in μm for TE modes for the half-quadratic potential well example. Values in the second column are obtained by the asymptotic formula (11) whereas values in the third column are obtained by our Finite Difference program.

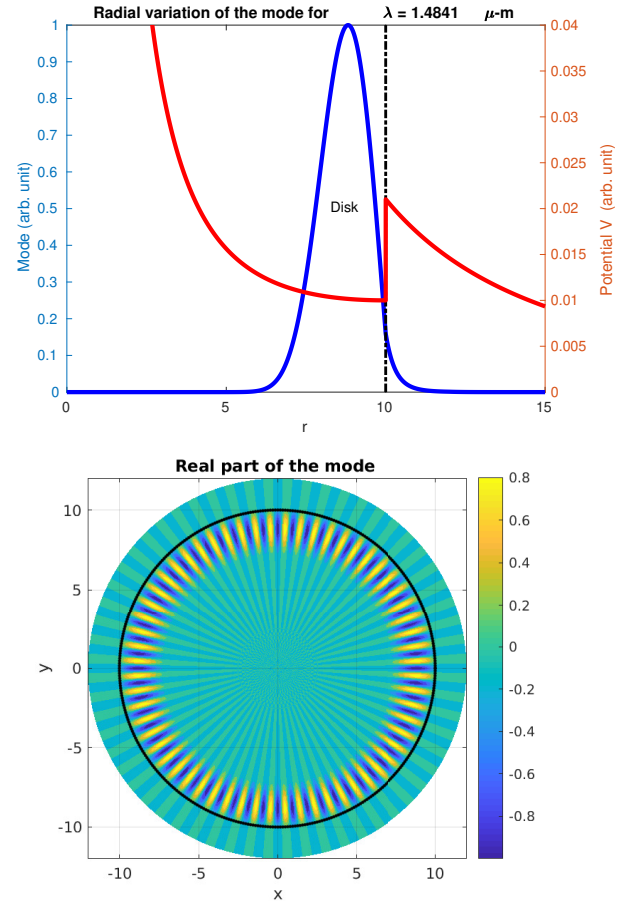


Fig. 3. Variation in the radial direction of the modulus of the mode u_m for the first resonance provided in Table 4 (top, blue line), potential V (top, red line) and 2D representation of the real part of $u_m(r)e^{im\theta}$ (bottom, the black circle indicates the disk boundary, the PML area is not represented).

creasing sequence of the zeros of the reverse Airy's function) and in Table 4 can be interpreted as the number of sign changes (or nodal points) of the real part of a mode inside the cavity.

3.3 Quadratic potential well

Finally, we consider the case of a micro-disk with radius $R = 10 \mu\text{m}$ and refractive index varying according to the radial position r as $n(r) = n_0 + \frac{1}{2}n_2(R^2 - r^2)$ where $n_0 = n(R) = 1.45$

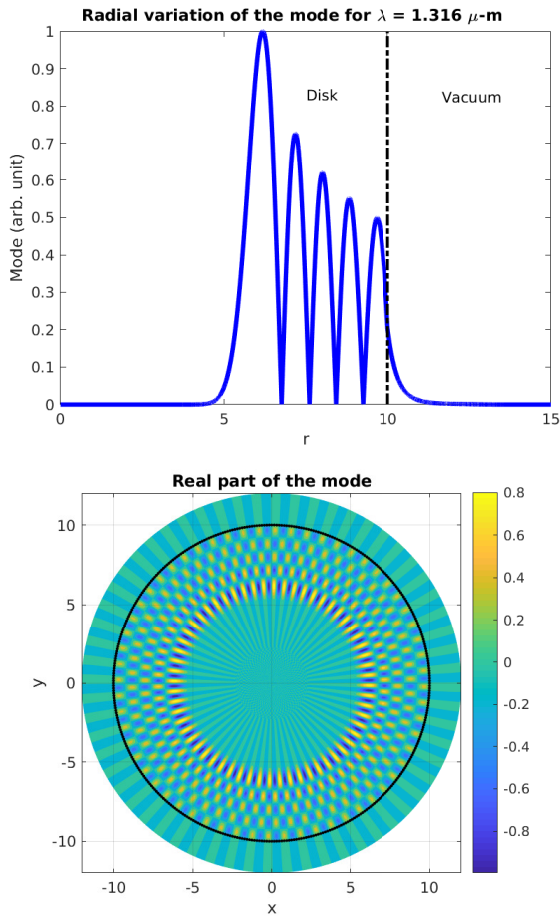


Fig. 4. Variation in the radial direction of the modulus of the mode u_m for the fifth resonance provided in Table 4 (top) and 2D representation of the real part of $u_m(r)e^{im\theta}$ (bottom; the black circle indicates the disk boundary, the PML area is not represented).

and $n_2 = 0.031 \mu\text{m}^{-2}$. This refractive index profile is similar to the quadratic-index glass doped with dye molecules studied in [6]. We have $\kappa = \frac{1}{R}(1 - \frac{n_2 R^2}{n_0}) < 0$. This refractive index profile falls into the quadratic potential well case. The potential V has a unique minimum inside $[0, R]$ located at $R_0 = \sqrt{\frac{2n_0 + n_2 R^2}{3n_2}}$.

We provide in Table 5 the first five resonance wavelengths λ in μm for TE modes with polar mode index $m = 60$ obtained by the asymptotic formula (17) (second column) and computed by our Finite Difference program (third column) with a step-size of $10^{-3} \mu\text{m}$.

We have depicted in Fig. 5 the variations in the radial direction of the modulus of the mode u_m for the first resonance provided in Table 5 (top) and the 2D representation of the real part of $u_m(r)e^{im\theta}$ (bottom). This illustrates the possibility with certain profiles of graded index to shift of the spatial location of WGM away from the exterior surface of the resonator towards the interior of the resonator reducing the overall optical losses.

1	1.6583228	$1.6586734 + i6.2523027 \cdot 10^{-15}$
2	1.6124380	$1.6125508 + i5.8994609 \cdot 10^{-14}$
3	1.5690241	$1.5684167 + i2.6968034 \cdot 10^{-13}$
4	1.5278866	$1.5257651 + i7.0206468 \cdot 10^{-13}$
5	1.4888512	$1.4843304 + i5.2191255 \cdot 10^{-13}$

Table 5. First five resonance wavelengths λ in μm for TE modes for the quadratic potential well example. Values in the second column are obtained by the asymptotic formula (17) whereas values in the third column are obtained by our Finite Difference program.

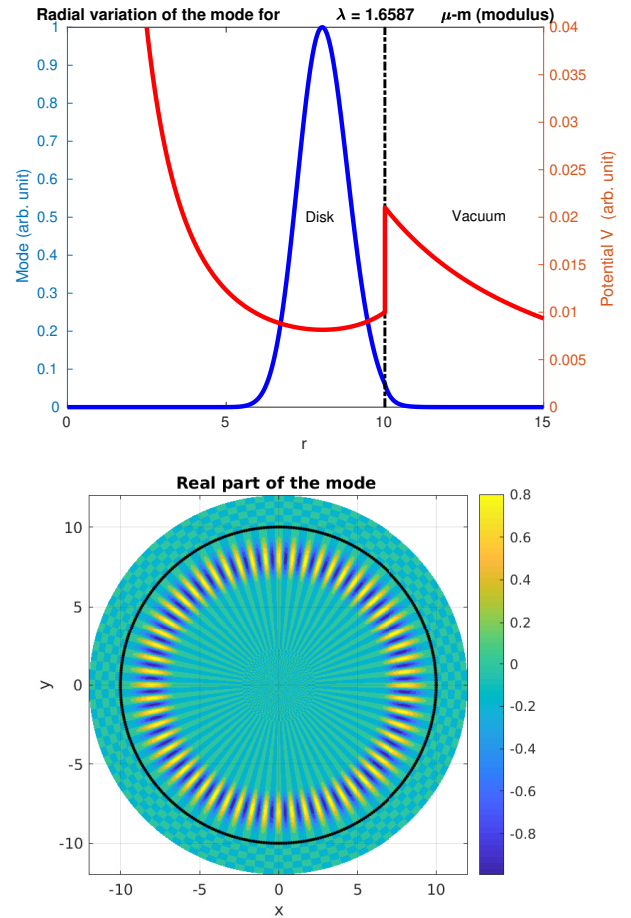


Fig. 5. Variation in the radial direction of the modulus of the mode u_m for the first resonance provided in Table 5 (top, blue line), potential V (top, red line) and 2D representation of the real part of $u_m(r)e^{im\theta}$ (bottom). The black circle indicates the disk boundary. The PML area is not represented.

4 Conclusion

We have investigated WGM in a graded index micro-disk where the refractive index n varies with the radial position r and we have highlighted three different behaviors for the WGM depending on the sign of a key parameter found to be $\kappa = \frac{1}{R} + \frac{n_1}{n_0}$ where n_0 and n_1 are respectively the values of the refractive index and its derivative at the cavity boundary. Moreover, we have obtained asymptotic expansions of the resonances for large polar mode index m aimed at providing first-approximation

of WGM in a graded index micro-disk in a simple and quick way.

Our approach has highlighted and quantified through our asymptotic formulas two interesting features of WGM in radially varying index micro-disks. In the half-quadratic potential well and in the quadratic potential well cases we have shown that the resonances are organized in an asymptotic lattice with constant steps along the modal index m and along the radial index j . We have also shown that in the quadratic potential well case, modes are slightly shift inside the cavity reducing their sensitivity to edge roughness.

Developing the approach whose first step is presented here, it is actually possible to obtain more terms in the asymptotic expansion of the resonances, but the mathematical technicality increases and formal calculus becomes necessary to make formulas explicit and usable, see [8,9]. Simple closed-form asymptotic formulas as the one derived in this paper already provide valuable insights on the properties of GRIN micro-disks. For instance, asymptotic formulas obtained in cases b and c show that equidistant spectrum can be obtained for a wide range on GRIN micro-disk with a step that has been made explicit. Such asymptotic formulas are complementary to a pure numerical simulation approach.

Finally, we would like to mention that the mathematical approach presented here can be adapted to apply to dielectric micro-spheres with a refractive index varying in the radial direction. Actually, as shown in Appendix C, TE resonances in the sphere can even be directly deduced from the asymptotics of TM resonances in the disk. Only the case of TM resonances in the sphere requires a specific study.

A TE and TM modes in a graded index optical micro-disk

For a WGM, the electric field \mathcal{E} and magnetic field \mathcal{H} have a sinusoidal variation in time represented in phasor notation as

$$\begin{aligned}\mathcal{E}(\mathbf{x}, t) &= \Re \left(\mathbf{E}(\mathbf{x}) e^{-i\omega t} \right) \\ \mathcal{H}(\mathbf{x}, t) &= \Re \left(\mathbf{H}(\mathbf{x}) e^{-i\omega t} \right)\end{aligned}$$

where ω denotes the optical wave frequency. This frequency is not imposed by sources but it is one of the unknown of the resonance problem with \mathbf{E} and \mathbf{H} . In the sequel we denote by Ω the domain occupied by the dielectric cavity which size typically varies from one to hundred micrometers and by Ω_e the exterior domain. The electric field \mathbf{E} and magnetic field \mathbf{H} are complex valued solutions to the harmonic Maxwell's equations in \mathbb{R}^3 :

$$\mathbf{curl} \mathbf{E} - i\omega\mu_0 \mathbf{H} = \mathbf{0} \quad (19a)$$

$$\operatorname{div} \mathbf{H} = 0 \quad (19b)$$

$$\operatorname{div} (\varepsilon_r \mathbf{E}) = 0 \quad (19c)$$

$$\mathbf{curl} \mathbf{H} + i\omega\varepsilon_0 \varepsilon_r \mathbf{E} = \mathbf{0} \quad (19d)$$

where μ_0 and ε_0 denote respectively the magnetic permeability and the dielectric permittivity of vacuum and ε_r denotes the relative dielectric permittivity of the dielectric material in the

cavity. Equations (19) can be handled in \mathbb{R}^3 when \mathbf{E} and \mathbf{H} refer to Schwartz's distributions or as regular functions in Ω and Ω_e with the following conditions at the interface between the two domains:

$$[\mathbf{H} \cdot \mathbf{v}] = 0 \quad [\varepsilon_r \mathbf{E} \cdot \mathbf{v}] = 0 \quad (20a)$$

$$[\mathbf{H} \wedge \mathbf{v}] = \mathbf{0} \quad [\mathbf{E} \wedge \mathbf{v}] = \mathbf{0} \quad (20b)$$

where \mathbf{v} denotes the unit outward normal to the boundary of Ω , and the brackets refer to the jump across the interface of the quantity inside the brackets. We also need to specify some condition at infinity for \mathbf{H} and \mathbf{E} .

By taking the curl of equation (19a) and combining it with equation (19d) we obtain

$$\mathbf{curl} \operatorname{curl} \mathbf{E}(x) - k^2 n^2(x) \mathbf{E}(x) = \mathbf{0}$$

where $k^2 = \omega^2 \mu_0 \varepsilon_0$ and n is the refractive index function defined by $\varepsilon_r(x) = n^2(x)$. From (19c) and the vector identity $\operatorname{div} (\varepsilon_r \mathbf{E}) = \varepsilon_r \operatorname{div} \mathbf{E} + \mathbf{E} \cdot \nabla \varepsilon_r$, we deduce that

$$\operatorname{div} \mathbf{E} = -\frac{\nabla n^2}{n^2} \cdot \mathbf{E}.$$

Then, using the vector identity $\mathbf{curl} \operatorname{curl} \mathbf{E} = -\Delta \mathbf{E} + \nabla \operatorname{div} \mathbf{E}$, where Δ refers to the vector Laplace operator, we finally obtain the following propagation equation

$$\Delta \mathbf{E} + \nabla \left(\mathbf{E} \cdot \frac{\nabla n^2}{n^2} \right) + k^2 n^2 \mathbf{E} = \mathbf{0}. \quad (21)$$

Similarly, by taking the curl of equation (19d) and by using the vector identity

$$\mathbf{curl} (\varepsilon_r \mathbf{E}) = \varepsilon_r \mathbf{curl} \mathbf{E} + \nabla \varepsilon_r \wedge \mathbf{E}$$

and equation (19a), we obtain that

$$-\mathbf{curl} \operatorname{curl} \mathbf{H} + \frac{\nabla n^2}{n^2} \wedge \operatorname{curl} \mathbf{H} + k^2 n^2 \mathbf{H} = \mathbf{0}.$$

Since \mathbf{H} is divergence free, the propagation equation for \mathbf{H} also reads

$$\Delta \mathbf{H} + \frac{\nabla n^2}{n^2} \wedge \operatorname{curl} \mathbf{H} + k^2 n^2 \mathbf{H} = \mathbf{0}. \quad (22)$$

As the dielectric micro-cavity is a disk with a radial varying refractive index n , it is quite natural to exploit this feature by introducing the cylindrical coordinates basis (r, θ, z) . In the cylindrical vector basis $(\mathbf{e}_r, \mathbf{e}_\theta, \mathbf{e}_z)$, we have

$$\frac{\nabla n^2}{n^2} = \frac{2}{n} \partial_r n(r) \mathbf{e}_r = \partial_r (\ln(n^2)) \mathbf{e}_r.$$

Considering the expression of the vector Laplace operator in cylindrical coordinates, component-wise the propagation equation (21) for \mathbf{E} reads

$$\begin{aligned}\Delta E_r - \frac{2}{r^2} \partial_\theta E_\theta - \frac{1}{r^2} E_r + \partial_r E_r \partial_r (\ln(n^2)) \\ + E_r \partial_r^2 \ln(n^2) + k^2 n^2 E_r = 0\end{aligned} \quad (23a)$$

$$\begin{aligned}\Delta E_\theta + \frac{2}{r^2} \partial_\theta E_r - \frac{1}{r^2} E_\theta + \frac{1}{r} \partial_\theta E_r \partial_r (\ln(n^2)) \\ + k^2 n^2 E_\theta = 0\end{aligned} \quad (23b)$$

$$\Delta E_z + \partial_z E_r \partial_r (\ln(n^2)) + k^2 n^2 E_z = 0 \quad (23c)$$

where Δ refers to the scalar Laplace operator.

Similarly, component-wise the propagation equation (22) for \mathbf{H} reads

$$\Delta H_r - \frac{2}{r^2} \partial_\theta H_\theta - \frac{1}{r^2} H_r + k^2 n^2 H_r = 0 \quad (24a)$$

$$\begin{aligned} \Delta H_\theta + \frac{2}{r^2} \partial_\theta H_r - \frac{1}{r^2} H_\theta - \frac{1}{r} \partial_r (\ln(n^2)) \partial_r (r H_\theta) \\ + \frac{1}{r} \partial_r (\ln(n^2)) \partial_\theta H_r + k^2 n^2 H_\theta = 0 \end{aligned} \quad (24b)$$

$$\begin{aligned} \Delta H_z + \partial_r (\ln(n^2)) (\partial_z H_r - \partial_r H_z) \\ + k^2 n^2 H_z = 0 \end{aligned} \quad (24c)$$

The main assumption in the model is that the electromagnetic field does not depend on the height variable z and the 3D geometrical problem setting can be reduced to a 2D one. This assumption and the resulting 2D problem can be seen as an approximation of the 3D one resulting from the use of the Effective Index Method [18].

Under the assumption that the magnetic field doesn't depend on the height variable z , the magnetic field component satisfies the following equation deduced from (24c)

$$\Delta H_z - \partial_r (\ln(n^2)) \partial_r H_z + k^2 n^2 H_z = 0$$

and this equation can be recast into

$$\operatorname{div} \left(\frac{1}{n^2} \nabla H_z \right) + k^2 H_z = 0.$$

Once H_z is known, the components E_r and E_θ of the electric field can be deduced from Maxwell's equation (19d). Namely,

$$E_r(r, \theta) = \frac{i}{\omega \epsilon} \frac{1}{r} \partial_\theta H_z(r, \theta), \quad (25a)$$

$$E_\theta(r, \theta) = -\frac{i}{\omega \epsilon} \partial_r H_z(r, \theta). \quad (25b)$$

Moreover, we deduce from the boundary conditions (20b) combined with (25b) that H_z satisfies the following interface conditions across the cavity boundary

$$[H_z] = 0, \quad \left[\frac{1}{n^2} \frac{\partial H_z}{\partial \nu} \right] = 0.$$

Similarly, (23c) can be recast into

$$\Delta E_z + k^2 n^2 E_z = 0.$$

and, under the assumption that the electromagnetic field doesn't depend on the height variable z , the components H_r and H_θ of the magnetic field can be deduced from Maxwell's equation (19a) as

$$H_r(r, \theta) = \frac{1}{i \omega \mu_0} \frac{1}{r} \partial_\theta E_z(r, \theta) \quad (26a)$$

$$H_\theta(r, \theta, z) = -\frac{1}{i \omega \mu_0} \partial_r E_z(r, \theta). \quad (26b)$$

Moreover, we deduce from the boundary conditions (20b) combined with (26b) that E_z satisfies the following interface conditions across the cavity boundary

$$[E_z] = 0, \quad \left[\frac{\partial E_z}{\partial \nu} \right] = 0.$$

Thus, Maxwell's equations in polar coordinates split into two independent subsystems of equations. The first one involves the electromagnetic field components H_z , E_r and E_θ and it is referred as the TE modes subsystem. The second one involves the electromagnetic field components E_z , H_r and H_θ and it is referred as the TM modes subsystem.

B Quantum mechanical analogy for a micro-disk cavity with constant index

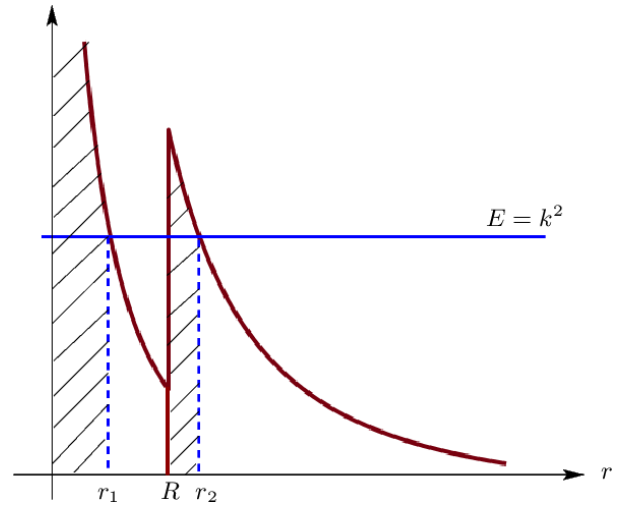


Fig. 6. Typical behavior of the potential function V_{eff} for disk cavity with constant index. The hatched area is the “classically forbidden” region.

We present in this appendix the quantum mechanical analogy for resonances in a disk cavity with constant index, see also [19,20]. For a disk cavity with constant index n_0 , Schrödinger equation (4) can be recast for the purpose of the interpretation, in the form of

$$-\mathcal{L}u_m(r) + V_{\text{eff}}(r)u_m(r) = E u_m(r) \quad (27)$$

where linear differential operator \mathcal{L} reads for $n \equiv \text{cste}$

$$\mathcal{L} = \partial_{rr}^2 + \frac{1}{r} \partial_r,$$

the effective potential V_{eff} is

$$V_{\text{eff}}(r) = k^2(1 - n^2(r)) + \frac{m^2}{r^2}$$

and the energy E is defined as k^2 , where k is assumed to be a positive real number for the purpose of the analogy. The effective potential is the sum of the dielectric potential $k^2(1 - n^2(r))$ and the repulsive centrifugal potential m^2/r^2 . It has the form of a half-triangular potential well as shown in Fig. 6.

By comparison to quantum mechanics, a noteworthy difference is that the effective potential function depends on the

energy $E = k^2$, whereas in quantum mechanics the potential is usually a fixed function, independent of the energy. As a consequence, the depth of the well gets deeper when k is raised whereas in quantum mechanics the depth of the well remains fixed as the energy of the particle changes.

By using the substitution $\zeta = \ln(kr)$, equation (27) reads

$$u_m''(\zeta) + q_m^2(\zeta) u_m(\zeta) = 0 \quad (28)$$

where $q_m^2(r) = r^2(E - V_{\text{eff}}(r))$ can be interpreted as an effective wave-number. The effective wave number q_m^2 has two zeros, the *classical turning points*, $r_1 \in]0, R[$ and $r_2 \in [R, +\infty[$. They are found to be $r_1 = m/(kn_0)$ and $r_2 = m/k$. They define two regions: the *classically forbidden* one $]0, r_1[\cup]R, r_2[$ where $q_m^2 < 0$ and the *classically allowed* one $[r_1, R] \cup [r_2, +\infty[$ where $q_m^2 > 0$.

In the quantum mechanical analogy a particle can tunnel through the classically forbidden region $]R, r_2[$ into the classically allowed one. For certain values of the energy (corresponding to the resonances) the particle becomes temporally trapped in the well, oscillating back and forth before finally tunneling back through the classically forbidden region to the outside region. Note that the solutions to the Schrödinger equation (28) are found to be a linear combination of Bessel's functions in the form $u_m(r) = C_1 J_m(nkr) + C_2 Y_m(nkr)$ (where $n = n_0$ if $r < R$ and $n = 1$ if $r > R$). It follows from the properties of Bessel's functions [14] that when $nkr > m$, i.e. when $q_m^2 > 0$, the "classically allowed" solutions exhibit an oscillatory behavior whereas when $nkr < m$, i.e. when $q_m^2 < 0$, the "classically forbidden" solutions show an exponential decaying behavior. Therefore, "classically allowed" solutions exist whenever k^2 exceeds the effective potential V_{eff} . This justifies the interpretation of V_{eff} as defining a well that separates the propagating solutions inside and outside by a tunnel barrier.

As the energy $E = k^2$ is reduced in value, the bottom of the potential well will be reached and for some value k_{\min} of k the energy E will coincide with the bottom $V_{\text{eff}}(R^-) = \lim_{r \nearrow R} V_{\text{eff}}(r)$ of the potential well. It is found that $k_{\min} = m/(n_0 R)$. There is no solution below the bottom of the well. On the contrary, as k is raised in value, the energy $E = k^2$ will eventually coincide with the top $V_{\text{eff}}(R^+) = \lim_{r \searrow R} V_{\text{eff}}(r)$ of the well for some value k_{\max} of k found to be $k_{\max} = m/R$. Solutions above the top of the well are generally not considered to be resonances. Thus, we have obtained that the real approximate values of the resonances are asymptotically located in the range between $\frac{m}{n_0 R}$ and $\frac{m}{R}$. Note that the tunnel barrier gets higher with increasing angular momentum m , which is a first indication that the whispering gallery modes propagating close to the dielectric interface have especially long lifetimes. If the refractive index n_0 is changed, the barrier top $V_{\text{eff}}(R^+)$ remains the same, but the well bottom $V_{\text{eff}}(R^-)$ grows deeper, so that the lowest allowed k will give rise to a higher quality factor.

C TE modes in a graded index micro-sphere: Ichenko and al. [7] work revisited

Let S be a sphere of radius R filled by a dielectric material with a radially varying refractive index $n = n(r)$. Scattering resonances in the TE mode case are considered in [7] under the

assumption that the relative electric permittivity $\varepsilon = n^2$ follows an affine law with r :

$$\varepsilon(r) = \varepsilon_0 + \varepsilon'(R - r), \quad \text{with } \varepsilon_0 > 1, \varepsilon' > 0. \quad (29)$$

The electric field \mathbf{E} in the spherical basis reads $\mathbf{E}(r, \theta, \varphi) = \frac{1}{r} \Psi(r) \mathbf{Y}_{\nu\mu}(\theta, \varphi)$ with $\mathbf{Y}_{\nu\mu}$ denoting vector spherical functions [7]. The equations satisfied by the radial function Ψ are found to be

$$\Psi''(r) + \left(k^2 n^2 - \frac{\nu(\nu+1)}{r^2} \right) \Psi(r) = 0 \quad (30a)$$

$$[\Psi(R)] = 0 \quad (30b)$$

$$[\Psi'(R)] = 0 \quad (30c)$$

$$\Psi(r) \propto \sqrt{r} H_{\nu+\frac{1}{2}}^{(1)}(kr) \text{ as } r \rightarrow +\infty. \quad (30d)$$

Note that eq. (30a) is set in [7] and that the radiation condition (30d) is classical in Mie scattering.

Then if we set

$$p = 1, \quad m = \nu + \frac{1}{2} \quad \text{and} \quad u_m(r) = r^{-\frac{1}{2}} \Psi(r) \quad (31)$$

we deduce from an elementary calculation that u_m solves the system of equations (3) with the same resonance k . The consequence of this fact is a straightforward translation of all our TM asymptotic formulas to the TE resonances of the sphere.

The affine law (29) writes $n(r) = (\varepsilon_0 + \varepsilon'(R - r))^{\frac{1}{2}}$. So our quantities n_0, n_1 in (7), and n_2 in (8) are given by

$$n_0 = \sqrt{\varepsilon_0}, \quad n_1 = -\frac{1}{2} \varepsilon' n_0^{-1}, \quad n_2 = -\frac{1}{4} (\varepsilon')^2 n_0^{-3}. \quad (32)$$

Now, our discriminant quantity κ introduced in (7) is given by

$$\kappa = \frac{1}{R} - \frac{\varepsilon'}{2\varepsilon_0}. \quad (33)$$

Hence, in accordance with [7], the three cases of potential well a), b), or c) can occur depending if $R\varepsilon'/2\varepsilon_0$ is smaller, equal or larger than 1, respectively. Our two-term asymptotics (11), (15), and (17), then yield formulas for the TE resonances of the sphere with polar mode index $\nu \in \mathbb{N}$, as follows.

a) $R\varepsilon'/2\varepsilon_0 < 1$. Recalling that $\check{\kappa}$ is defined as $R\kappa$, we obtain:

$$k_{\nu,q} = \frac{1}{R\sqrt{\varepsilon_0}} \left(\nu + 2^{-\frac{1}{3}} \left(1 - \frac{R\varepsilon'}{2\varepsilon_0} \right)^{\frac{2}{3}} a_q \nu^{\frac{1}{3}} + \mathcal{O}(1) \right) \quad (34)$$

which coincides with [7, eq. (13)].

b) $R\varepsilon'/2\varepsilon_0 = 1$. We have introduced μ in (8) and $\check{\mu} = R^2\mu$ is now given by

$$\check{\mu} = 2 + \left(\frac{R\varepsilon'}{2\varepsilon_0} \right)^2 = 3. \quad (35)$$

Since this quantity is positive, formula (15) is valid and gives

$$k_{\nu,q} = \frac{1}{R\sqrt{\varepsilon_0}} \left(\nu + \frac{4q+3}{2} \sqrt{3} + \frac{1}{2} + \mathcal{O}(m^{-\frac{1}{2}}) \right) \quad (36)$$

c) $R\varepsilon'/2\varepsilon_0 > 1$. Recall that the potential V in the radial variable r is the function

$$r \mapsto \frac{n_0^2}{r^2 n(r)^2} = \frac{\varepsilon_0}{r^2 (\varepsilon_0 + \varepsilon'(R - r))}.$$

Its derivative is proportional to $\varepsilon' r - 2(\varepsilon_0 + \varepsilon'(R - r))$ up to a positive factor. It cancels at the value $r = R_0$ given by

$$R_0 = \frac{2}{3} \left(R + \frac{\varepsilon_0}{\varepsilon'} \right).$$

It is easy to check that $R_0 \in (\frac{2}{3}R, R)$ and that

$$\ddot{\mu} = 2 + \left(\frac{R_0 \varepsilon'}{2\varepsilon(R_0)} \right)^2 = 3.$$

Thus formula (17) is valid and gives

$$k_{v,q} = \frac{1}{R_0 \sqrt{\varepsilon_0}} \left(v + \frac{2q+1}{2} \sqrt{3} + \frac{1}{2} + \mathcal{O}(m^{-\frac{1}{2}}) \right) \quad (37)$$

We can see that, as announced in [7], in the half-harmonic and harmonic cases b) and c), the resonances are distributed on an approximate lattice.

In contrast with what precedes, asymptotic formulas for TM resonances in the sphere cannot be directly deduced from the asymptotics of TE resonances in the disk; A specific analysis, similar to the one detailed in the paper for a disk, must be carried out. This observation can be seen already for a constant refractive index $n \equiv n_0$ by comparing our 4-term expansion (12) with [21, eq. (1.1)]: While all factors coincide for TE modes in the sphere when $p = 1$, the fourth ones are distinct for TM modes in the sphere when $p = -1$.

D Authors contributions

All the authors contributed equally to the study.

References

1. K. Vahala, *Optical Microcavities*, Advanced series in applied physics (World Scientific, 2004)
2. J. Heebner, R. Grover, T. Ibrahim, T. Ibrahim, *Optical Microresonators: Theory, Fabrication, and Applications* (Springer, 2008)
3. C. Gomez-Reino, M. Perez, C. Bao, *Gradient-Index Optics: Fundamentals and Applications* (Springer, 2002)
4. K. Dadashi, H. Kurt, K. Üstün, R. Esen, J. Opt. Soc. Am. B **31**, 2239 (2014)
5. Z. Najafi, M. Vahedi, A. Behjat, Opt. Commun. **374**, 29 (2016)
6. M.C. Strinati, C. Conti, Phys. Rev. A **90**, 043853 (2014)
7. V.S. Ilchenko, A.A. Savchenkov, A.B. Matsko, L. Maleki, J. Opt. Soc. Am. A **20**, 157 (2003)
8. S. Balac, M. Dauge, Z. Moitier, *Asymptotics for 2D whispering gallery modes in optical micro-disks with radially varying index* (2020), arXiv preprint 2003.14315
9. Z. Moitier, Ph.D. thesis, Université de Rennes, France (2019), tel.archives-ouvertes.fr/tel-02308978
10. M. Zworski, Notices Amer. Math. Soc **46**, 328 (1999)
11. J.F. Bony, N. Popoff, Asymptot. Anal. **112**, 23 (2019)
12. S. Ancey, A. Folacci, P. Gabrielli, J. Phys. A: Math. Gen. **34**, 1341 (2001)
13. J.W. Ryu, S. Rim, Y.J. Park, C.M. Kim, S.Y. Lee, Phys. Lett. A **372**, 3531 (2008)
14. M. Abramowitz, I.A. Stegun, *Handbook of Mathematical Functions: with Formulas, Graphs, and Mathematical Tables* (Dover Publications, 1965)
15. K. Kunz, R. Luebbers, *The finite difference time domain method for electromagnetics* (CRC Press, 1993)
16. S. Kim, J.E. Pasciak, Math. Comp. **78**, 1375 (2009)
17. J. Jin, *The finite element method in electromagnetics* (Wiley-IEEE Press, 2014)
18. K. Chiang, Opt. Lett. **16**, 714 (1991)
19. J. Nockel, Ph.D. thesis, Yale University, USA (1997)
20. J. Cho, I. Kim, S. Rim, G.S. Yim, C.M. Kim, Phys. Lett. A **374**, 1893 (2010)
21. C.C. Lam, P.T. Leung, K. Young, J. Opt. Soc. Am. B **9**, 1585 (1992)